Thickness Effect Analysis on Fatigue Crack Propagation of 7475 Plate Material under Variable Amplitude Loading

Jakub Šedek[1,*], *Roman* Růžek[1]

[1] VZLÚ – Czech Aerospace Research Centre, Beranových 130, Prague 9, 199 05, Czech Republic

Abstract. In the crack growth prediction models, the effect of variable amplitude loading is taken into account by different ways. One of them the Newman's model is used very often, but in its original form it is not able to take into account the effect of specimen thickness. The new modification which involves the specimen thickness is presented. The study of variable thickness impact is based on the FE – analysis of M(T) specimen. The variability of constrained factor α was analysed for several load levels and specimen thicknesses. The value of α is governed by the ratio of thickness B versus plastic zone size r_p. The effect of overloads on the plastic zone and relevant constraint factor value is analysed as well. During loading, it was found, that the constraint factor value is lower after overloads than when creating monotonic plastic deformation on the same load level in a large part of the cycle. The influence of thickness effect based on different α value after overload was successfully implemented into the strip yield model. Simulation of crack growth taking into account the thickness of the specimen under variable amplitude loading shows similar behaviour like the experimental data.

1 Introduction

Fatigue tests carried out under representative flight load spectra reveal different crack growth lives depending on the specimen thickness. Crack propagation for the thinnest sheet material is being up to 10 times longer than for the thick material in spite of no significant differences are observed under constant amplitude loading [1]. The clarification of different crack growth under variable amplitude loading can be explained by the Elber's concept of plasticity induced crack closure known since late sixties [2]. The increased thickness leads to more plane strain at the crack front and thus the smaller plastic zone is created resulting in smaller crack closure and less crack growth retardation. The influence of different thickness on the crack growth is related to the different out-of-plane plastic constraint at the crack tip [3, 4]. The out-of-plane constraint depends on the plastic zone size and the thickness of the specimen.

Nowadays, the damage tolerance philosophy is applied to design inspection service intervals of advanced airframe structures. Several fatigue crack growth prediction models

* Corresponding author: sedek@vzlu.cz

can be selected for this purpose. The effect of variable amplitude loading is taken into account by different ways. Elber's concept of plasticity induced crack closure represents the basic approach on which the one type of prediction models works – the strip yields models (SYM). The Newman's model [5] is used very often, but in its original form it is not able to take account for specimen thickness. Nevertheless, some attempts modifying SYM try it to implement [4, 6]. The modifications include the thickness dependency through the variable constraint factor α, which is correlated to the stress state at the crack tip. The plane stress, the plane strain or the transitional state between is evaluated based on the plastic zone size and the thickness.

The own modification similar to Guo [4] but enhanced by variable constraint factor α in dependence on the overload is introduced in this work.

2 Stress near the crack tip under cyclic loading

The effect of overloads on the plastic zone and relevant plastic constraint factor were analysed using FE-model of the central cracked specimen (M(T)) with dimensions of 100 x 80 x 20 mm and the half crack length of 20 mm. The analysis including pre/post-processing was carried out in FE-software package ABAQUS 2017. The model was represented by 1/8 portion using symmetry in three basic planes in order to simplify the analysis. For discretization 57 000 hexahedral elements of C3D8R type were used. Six layers of elements was used through the thickness of the model. Due to the symmetry applied, the total number of elements through the specimen thickness was twelve. The elastic-perfectly plastic material with isotropic hardening and yield stress of 500 MPa were assumed. The initial linear elasticity was characterized by Young's modulus E = 72 000 MPa and Poisson's ratio ν = 0.3. Material characteristics were used relating the aluminium alloys used in aerospace industry.

The stress and strain fields in cyclically loading material at the crack tip is different from the fields created by monotonic loading. Loading crack in virgin material creates plastic zone from the beginning and the size of plastic zone increases with power law. Contrary in the cyclically deformed material, the residual plastic zone is present and the forward plastic zone develops from the opening stress level.

The analysis of crack tip field was carried out for 100 cycles. Two stress conditions characterized by the ratio of the thickness B versus the plastic zone size r_p according to Irwin were evaluated. The conditions close to plane strain with $B/r_p^{Irwin} = 79$ and the plane stress with $B/r_p^{Irwin} = 7$ were analysed. The stress σ_{yy} ahead of the crack tip in the plane of the crack was normalized by yield stress $\sigma_{yield.}$ The results are shown in Fig. 1 in comparison with the maximum monotonic load stress determined in the first cycle. The normalized stress increases up to maximum value of 2.5 and then gradually decreases with the distance from the crack tip. The dot points in the figure denotes the plastically deformed elements.

The stress development after 100 cycles according to increasing the load shows the effect of cyclic loading. The stress ahead of the crack is decreased due to residual stress field, but at certain distance the influence is eliminated. The stress reduction is clearly seen behind the cyclic plastic zone (see Fig. 1a for plane strain condition). The increasing size of the plastic zone according to load level is obvious as well, but at the maximum load level the size is smaller than in the first cycle.

The plastic zone size under plane stress conditions is several times larger than under plane strain conditions (see Fig. 1b). The stress reduction after cyclic plastic zone is also present. At highest load levels after 100 cycles it can be seen the higher stress inside the plastic zone then in the first cycle.

For both stress state conditions, the stress reduction after the cyclic plastic zone is present in the area of the monotonic plastic zone created in the first cycle. The oscillations before the crack tip are caused by the used element types and are not relevant.

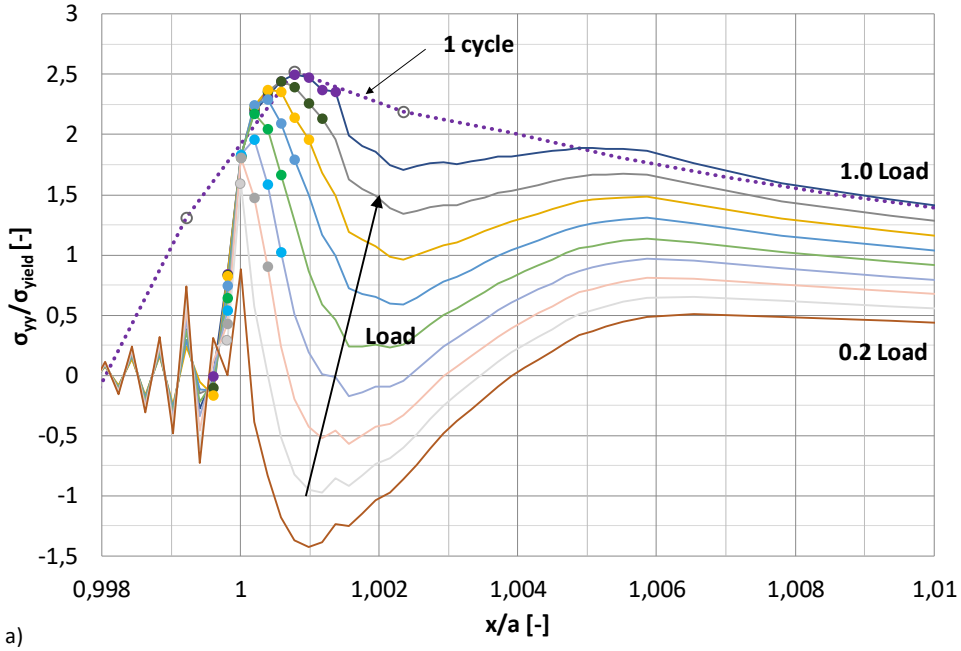

a)

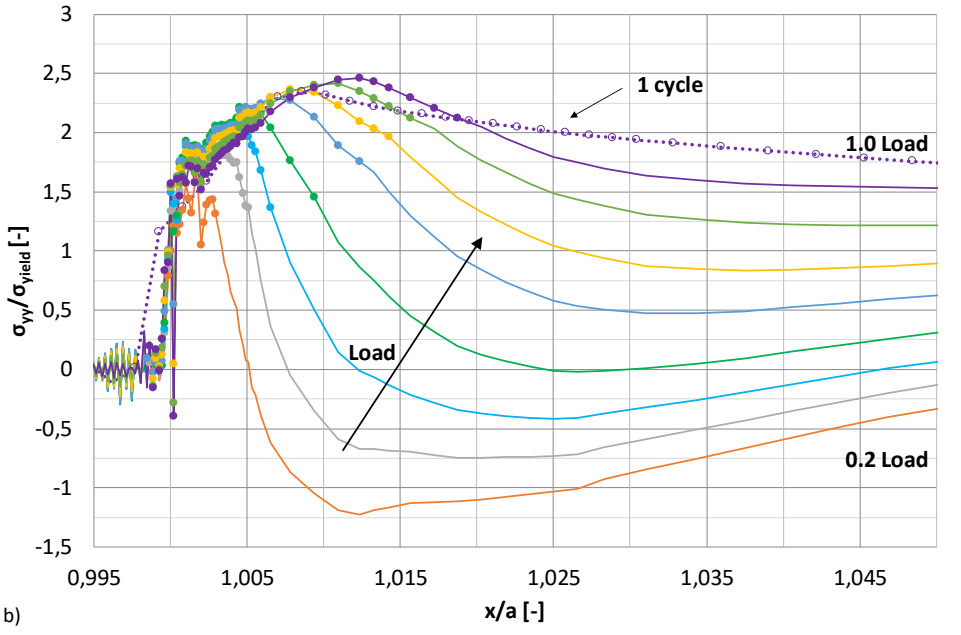

b)

Fig. 1. Normalized stress $\sigma_{yy}/\sigma_{yield}$ in the the crack plane after 100 cycles a) centre of the specimen $B/r_p^{Irwin} = 79$; b) sides of the specimen $B/r_p^{Irwin} = 7$.

2.1 Constraint factor

The out-of-plane plastic constraint reflecting the stress state conditions at the crack tip can be evaluated by many parameters [3 - 9]. The Newman's constraint factor α was chosen in this work. The factor α is defined in the plastic zone as the stress perpendicular to the crack plane σ_{yy} versus the flow stress σ_o by Eq. 1 The flow stress is assumed as the first approximation of stress-strain curve by the average of the strength σ_{Rm} and yield stress σ_{yield}.

$$\alpha = \frac{\sigma_{yy}}{\sigma_0}, \text{ where} \tag{1}$$

$$\sigma_0 = \frac{\sigma_{Rm} + \sigma_{yield}}{2} \tag{2}$$

In the case of flat specimen, the constraint is being evaluated through the whole thickness and the global factor α_g is defined as the weighted average through the plastic zone.

$$\alpha_g = \frac{1}{A}\iint \alpha da \tag{3}$$

A denotes normal cross-section area through yielded material in the uncracked ligament. When applying finite element analysis, the Eq. 3 can be expressed as Eq. 4.

$$\alpha_g = \frac{1}{A_T}\sum_{i=1}^{N}\left(\frac{\sigma_{yy}}{\sigma_0}\right)_i A_i \tag{4}$$

A_i denotes the area of yielded element i in the plane $y = 0$, σ_{yy}/σ_0 is the normalized normal stress in the element i and A_T is the area of all yielded N elements in the crack plane.

For monotonic loading represented by the first cycle, the sigmoidal relationship plotted in logarithmic coordinates was determined in dependence on the ratio of specimen thickness B versus the plastic zone size r_p in [10]. The shape of sigmoidal curve described by Eq. 5 depends on two parameters D and β and C governs the maximum value according to Poisson's ratio. The minimal value of α was determined 1.11. Eq. 5 can be used for local factor α and global factor α_g as well.

$$\alpha = 1.11 + \frac{\frac{1}{1-2\nu} - C}{1 + D\left(\frac{r_p}{B_{eq}}\right)^{\beta}} \tag{5}$$

The development of the constraint factor α_g during loading after 100 cycles was determined similarly as in [10] for the M(T) specimen 20 mm thick, but the different behaviour of α_g dependency was obtained (see Fig. 2). The constraint factor α_g initially increases with increasing load contrary to the monotonic loading without presence of residual plastic zone. The value of the constraint factor α_g at maximum load level is located close to the α_g curve obtained in the first cycle, but the values at lower load levels are far away of the α_g curve. The reason is the dependency on the plastic zone size determined according to Irwin, which is intended for monotonic loading. The cyclic loading leads to the cyclic plastic zone and so the values are shifted right in the graph. The constraint factor increases from the values close to plane stress conditions almost linearly, if shown in log-log scale, but before maximum load level the local extreme is present. The plastic zone under plane stress condition (lower part of the α curve) causes the drop of α_g to the α_g curve of monotonic loading at maximum load level, but toward to plane stress condition (upper part of the α_g curve) the drop is reduced. It seems in the graph, that the area of possible α_g values is bounded by the upper α_g curve denoted α_{CU} and lower α_g curve denoted α_{CL}.

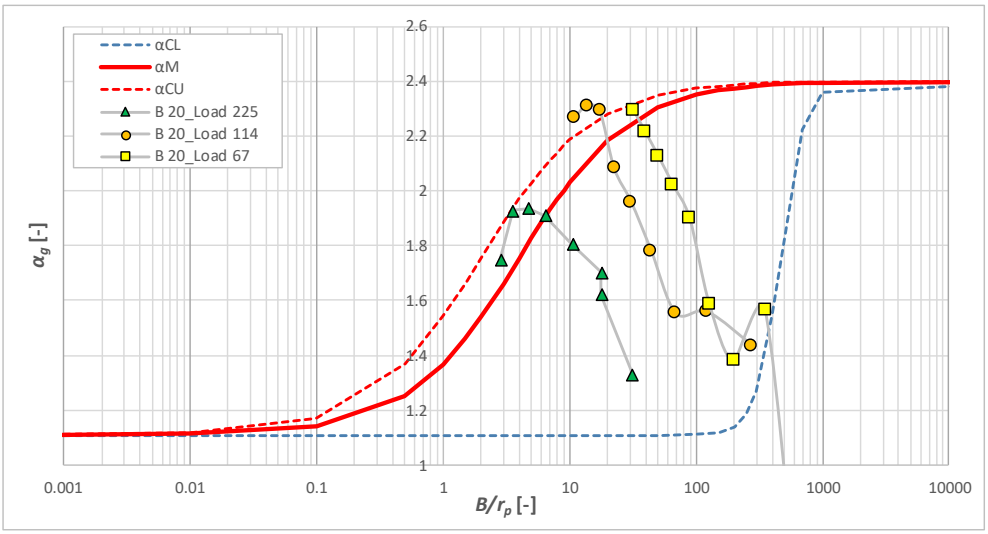

Fig. 2. Development of constraint factor α during increasing load level after 100 cycles for M(T) specimen 20 mm thick.

Since the Elber's phenomenon appears during cyclic loading, it is preferable to use load level related to opening stress S_{open}.. The normalized load was implemented by Eq. 6, where S denotes the load stress and S^{OL} is the overload. The overload level during cyclic loading with constant amplitude is the maximum load level in the cycles.

$$\phi = \frac{S - S_{open}}{S^{OL} - S_{open}} \tag{6}$$

The monotonic development of the expression involving α_g value can be found in dependence on ϕ by assuming the normalized difference (α_g - α_{CL}) introducing the parameter κ_1 via Eq. 7.

$$\kappa_1 = \frac{\left(\alpha_g - \alpha_{CL}\right)}{\left(\alpha_{CU} - \alpha_{CL}\right)} \tag{7}$$

Plot of κ_1 values for three load levels of the specimen 20 mm thick determined numerically in dependence on ϕ is shown in Fig. 3. The analytical approximation by Eq. 8 is shown in the figure as well.

$$\kappa_1 = \frac{\sin\left(\phi\pi/2\right) + \sqrt{\phi}}{2} \tag{8}$$

The development of constraint factor α_g during loading is then expressed via Eq. 9, where parameter κ_2 evaluates the position of the crack front in the plastic zone from overload. Subscript denotes the appropriate curve (M - monotonic, CU – cyclic upper, CL - cyclic lower). The constant parameter γ_2 controls the influence of κ_2 and the value of 3 is assumed in this work.

$$\alpha_g = \alpha_M - \left(\alpha_M - \left(\alpha_{CL} + \left(\alpha_{CU} - \alpha_{CL}\right)\sin\left(\kappa_1\pi/2\right)\right)\right)\left(1 - \kappa_2^{\gamma_2}\right) \tag{9}$$

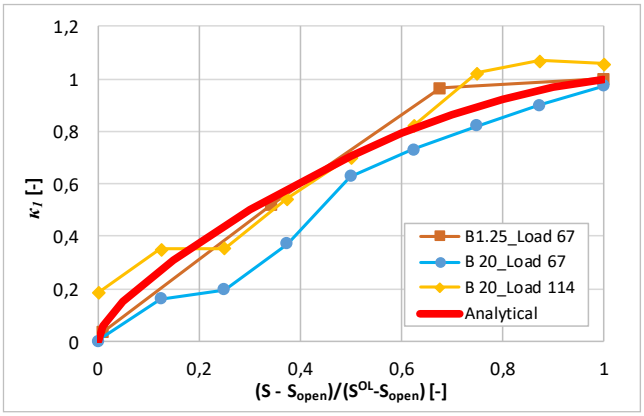

Fig. 3. Development of the parameter κ_1 during increasing load level after 100 cycles for M(T) specimen 20 mm thick; FE-results and analytical approximation.

3 Analysis of crack growth under variable amplitude loading

Usually, the crack is initially under plane strain conditions and as the crack develops the plastic zone size increases. The ratio of plastic zone size and the thickness of the specimen governs the conditions at the crack tip. Longer crack under sequence of variable amplitude loading can loss the constraint at high peaks and the plastic zone size became larger. Contrary, following underloads can clear the overload effect.

The influence of thickness was analysed on M(T) specimens made from aluminium alloy 7475-T7351 in L-T direction. The specimens were 250 mm long, 100 mm wide with thickness of 2, 4 or 8 mm. Fatigue crack growth tests were carried out using a hydraulic SCHENCK load frame with a capacity of 250 kN. The load frame was controlled by the INSTRON FastTrack 8800 test control system. It provides real-time closed loop control, including transducer conditioning and function generation. Specimens were clamped into the test frame using mechanical grips. The test procedure was conducted in agreement with the requirements of ASTM E-647 standard [11]. Fatigue crack initiation and propagation were monitored via a visual method (VT) using an Olympus SZ40 light stereomicroscope with a maximum magnification of 40x. Crack length measurements were carried out on both surfaces and sides relative to the longitudinal axes of the specimens.

Variable amplitude loading was realized by sequence of cycles representative for the lower wing panel of the commuter aircraft. The exceedance plot is shown in Fig. 3. The cycles with load ratio R in the range of (0.3 - 0.4) are most numerous. The experimental evaluation of crack growth was carried out on specimens with different thickness. The tests with constant amplitude loading at different load ratios were also conducted in order to determine material data of crack growth. The crack growth rate data were represented by Paris law in the form

$$\frac{\Delta a}{\Delta N} = C\Delta K_{eff}{}^{m}, \tag{10}$$

where $\Delta a/\Delta N$ denotes the crack growth rate and ΔK_{eff} is the amplitude of effective stress intensity factor. Coefficients $C = 1.92e\text{-}10$ and $m = 3.3$ are the characteristics of the crack growth rate curve. The dependency $\Delta a/\Delta N = f(\Delta K_{eff})$ was determined by processing crack growth data for different load asymmetry ratio R in the form $\Delta a/\Delta N = f(\Delta K(R))$. In this procedure the Newman's Crack Opening Stress Equation was employed [5].

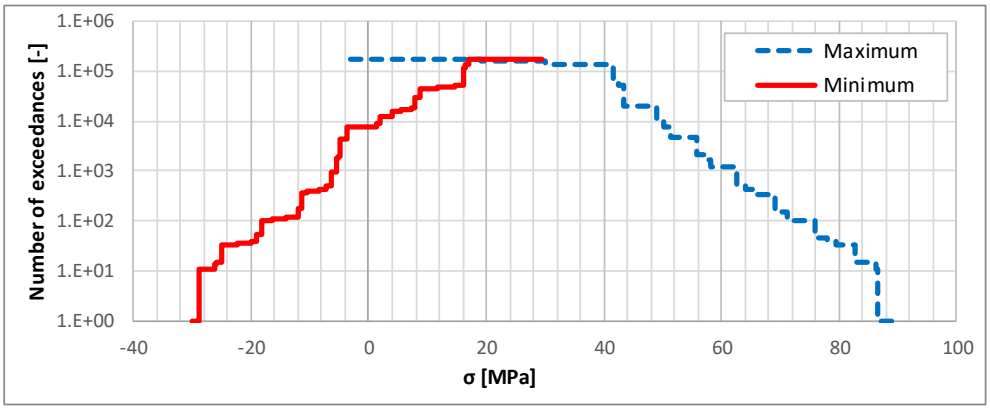

Fig. 3. Exceedance plot for variable loading sequences.

Implementing the relationships (5 - 9) into the SYM the simulations of crack growth were performed. The analysis of crack growth under constant amplitude loading revealed no severe differences between computed and experimentally determined specimen lives. During constant amplitude tests the thickness effect was not recognized. Applying the variable amplitude loading results in different experimental lives as shown in Fig. 4. The test and simulated crack growth curves showed very similar behaviour like plateau in crack growth rate for thinnest specimen. Generally, the thinner the specimen, the longer life was obtained. Simulated life of middle-thick 4 mm specimen was shorter then tested, but the difference was caused by higher crack growth rate during short crack. Original SYM model predicts well the 8 mm thick specimen with no difference seen in comparison with modified SYM model, but no thickness dependency occurred. The crack growth determined by original SYM was much more retarded with decreasing specimen thickness.

The simulations using modified SYM were carried out with little shift of lower part of the α monotonic curve toward to higher values of B/r_p than determined from FEM as shown in Fig. 2 in order to correctly characterize the retardation effect after single overload, as similarly found out in reference [5]. The constants values were used as follows: $D = 50$ and $\beta = 2$.

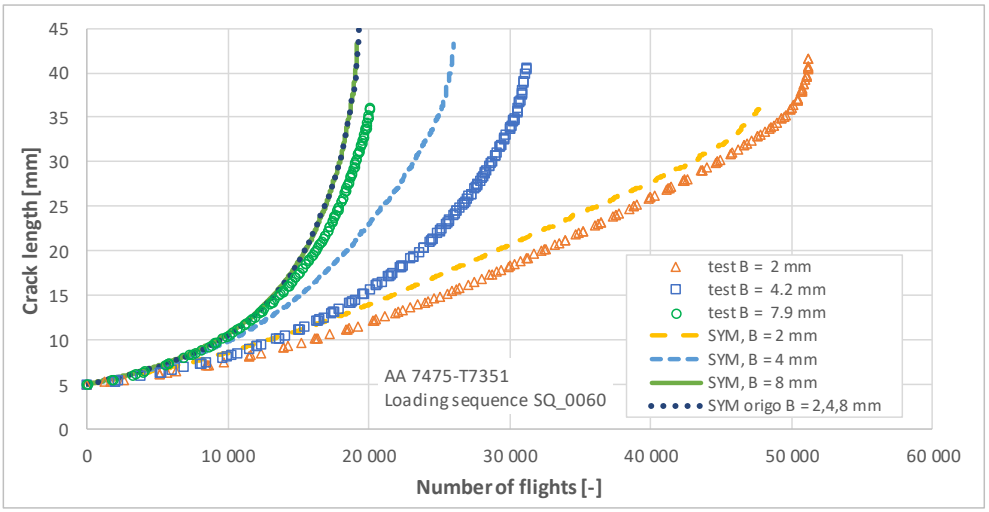

Fig. 4. Crack growth curves for test and simulation using original and modified SYM

4 Discussion and conclusions

The crack tip stress field during cyclic loading was analysed employing numerical method. The influence of residual stress on plastic zone development was found out significant causing the change of plastic constraint in comparison with monotonic loading. The constraint variability was implemented into the strip yield model (SYM) and the simulation of crack growth under variable amplitude loading was carried out for M(T) specimens from aluminium alloy 7475-T7351. Analyses showed similar simulated crack growth behaviour as the experimental data. The obvious plateau in crack growth rate was pretty captured on the thinnest specimen and it was shown that the thinner specimen yields longer crack growth life compared to the thicker one. From the plot of crack growth curves there can be seen longer cracks according to experimental observations. The reason could be assigned to greater crack growth rate at small amplitudes of stress intensity factor, especially at short crack. In the material data of crack growth only Paris law regime was described and no threshold value was assumed. Generally, modified SYM gave more realistic results than the original model that is non-sensitive to specimen thickness as was experimentally proved.

References

1. R. Růžek, P. Homola, M. Kakos, Trebuňa F. et al., (eds.). EAN 2017 - 55th Conference on Experimental Stress Analysis 2017: Conference Proceedings, May 30th – June 1st, 2017, Nový Smokovec, Slovakia, TU Košice – Faculty of ME, (2017) 760 pages, pp. 513-518; ISBN 978-80-553-3167-6
2. W. Elber, Damage Tolerance in Aircraft Structures. *ASTM STP 486*, (1971) pp. 230-242
3. W. Guo, Elsevier, 1999, *Engineering Fracture Mechanics* **62**, pp. 383-407
4. W. Guo, C.H. Wang and L.R.F. Rose, *Fatigue Fract. Eng. Mater. Struct.*, 1999, vol. 22, No. 5, pp. 437-444
5. J.C. Newman Jr., *International Journal of Fracture* **24**, No. 4, pp. 131- 135, (1984)
6. T. Machniewicz, *Mechanics and control*, 2012, vol.31, No.4, pp. 150-157
7. A. Materna, V. Oliva, Prague, CTU, Faculty of Nuclear Sciences and Physical Enginering, KMAT - FJFI, 1999, V-KMAT- 459/99
8. J. C. Newman Jr., C. A. Bigelow, K. N. Shivakumar, NASA LRC, 1993, NTM 107704
9. W. Guo, *Engineering Fracture Mechanics* **51**, No. 1, pp. 51-72 (1995)
10. J. Šedek, Trebuňa F. et al., (eds.). EAN 2017 - 55th Conference on Experimental Stress Analysis 2017: Conference Proceedings, May 30th – June 1st, 2017, Nový Smokovec, Slovakia, TU Košice – Faculty of ME, (2017) 760 pages, pp. 174-177; ISBN 978-80-553-3167-6
11. ASTM E 647-15e1: Standard Test Method for Measurement of Fatigue Crack Growth Rates, 2015.